



# Design approach of a density-driven solar water heater system

## A study in North Dakota

R. Shukla<sup>1</sup> · K. Sumathy<sup>1</sup>

Received: 15 April 2018 / Accepted: 6 September 2018 / Published online: 20 September 2018  
© Akadémiai Kiadó, Budapest, Hungary 2018

### Abstract

Energy conservation continues to play a crucial role in social and economic development. With the remarkable increase in oil prices and exploring solutions for the replacement of fossil fuels, an ecofriendly energy resource has become the priority among more and more people. Keeping the intension for reducing the global warming impact and looking for alternative clean source of energy, solar energy applications such as solar thermal systems, solar water heating and cooling are becoming energy-efficient designs. One of the widely used applications of solar energy is solar water heating systems. Low-cost solar water heaters can cover the domestic needs for water in the range of 100–200 l per day. Solar water heating systems are generally more efficient and advantageous in hot areas. However, the application of solar water heating is still a challenge in winter and sub-zero conditions, having low solar irradiance. In such conditions, solar water heating system cannot produce enough energy, which drives a need for evaluating system component design and improves its performance during low ambient conditions. In this study, detailed design methods for solar water heater components are discussed for cold regions like North Dakota, USA. The type of system chosen in this study is natural circulation-based solar water heating system. The study will also compare the experimental data with previously conducted numerical analysis.

**Keywords** Solar water heating · Natural circulation · Global warming · Ecofriendly

### Introduction

According to the Solar Energy Industries Association, there have been a tremendous growth to the solar sector since its initial passage in 2006. The average annual growth rate in solar energy was noticed to be 60%, in the last decade. Due to the continuous burning of fossil fuels and its large contribution toward global warming greenhouse effect, researchers, and industries are expanding their solar offerings and continue to innovate and redefine ability to use and store energy. The market linked with solar power is rising and in 2015, solar energy jobs in the USA increased by 22% in comparison with previous years. The USA formed the fifth largest market for solar thermal collectors

[1]. One of the many applications of solar energy is solar water heating (SWH). Low-cost solar water heaters can cover the domestic needs for water in the range of 100–200 l per day at low temperature (40–70 °C) [2]. Generally, solar water heating system operates more efficiently in hot or warm regions and generates more hot water compared to colder regions. While utilizing a solar water heating system in cold climate area, there have been several challenges noticed due to low solar insolation, low ambient temperatures and high heat loss from the panel [3, 4]. Therefore, it is always hard to harness solar energy, when it is below freezing outside and the sunlight is weak.

An attempt has been made in this study, to discuss the design aspects of SWH system and its components which can effectively harness the solar energy for water heating purposes in low ambient conditions (such as North Dakota). The study will demonstrate the storage tank, heat exchanger and collector design for harsh climate conditions. The experiments were conducted to evaluate the characteristics of a supercritical CO<sub>2</sub>-based solar collector,

✉ R. Shukla  
itruchi@gmail.com

<sup>1</sup> Department of Mechanical Engineering, North Dakota State University, Fargo, ND 58108-6050, USA

including CO<sub>2</sub> temperature and pressure (for North Dakota weather conditions), and are presented in this paper.

## Experimental setup design

This study demonstrates a simple design of thermosyphon SWH which has been equipped to work in harsh winter condition, found in regions like Fargo, ND. Below sections will describe the individual component design for a simple thermosyphon system for harsh climate conditions.

### Hot water storage tank

The correct design of a storage tank can positively improve the performance of an entire cooling/heating system. In this study, a thermally effective storage tank was designed to store water from a solar powered collector having an exposed gross area of 1.15 m<sup>2</sup>. A steel storage tank was used as they are easy to install and corrosion free [5].

In addition to the material type, there are other design factors such as storage tank configuration and tank size that influence the performance of the storage tank. In this study, a vertically oriented storage tank was utilized because of its superior thermal performance compared to horizontal geometry [5].

While defining the tank size, an aspect ratio, i.e., height/diameter of the tank plays a significant role in establishing the overall heat loss coefficient. Tank's overall heat loss coefficient increases with the increase in aspect ratio to the surrounding. This shows more surface area for the given volume of the tank. In order to achieve minimal heat losses from the tank (Table 1), an aspect ratio should be 2–4 [6]. Using these facts, a storage tank (Fig. 1) having a volume of 60 L and an aspect ratio of around 2 was fabricated. The methodology adopted in arriving at the volume of the tank is presented below.

### Determination of storage tank volume

The tank volume was determined by using the weather data of Fargo, ND region and evacuated tube collector (ETC) as the heat design. Since it is intended to operate the SWH system on thermosyphon basis (density-driven),

**Table 1** Relation between diameter and height of the storage tank

<i>D</i> /in.	<i>H</i> /in.	( <i>H</i> / <i>D</i> ) Aspect ratio
14	23	1.6
13	28	2.1
12	32	2.6

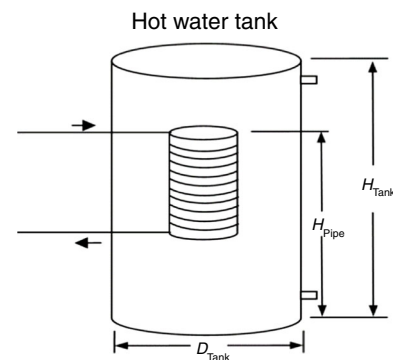
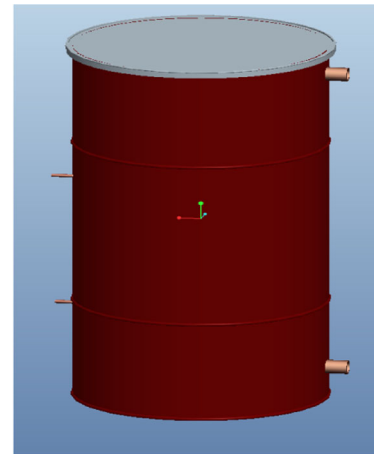


**Fig. 1** Picture and schematic of the designed storage tank

preliminary calculations showed that the system could not affect any useful heat in the harsh winter condition. Hence, the average hourly total radiation ( $I_T$ ) and the ambient temperature ( $T_a$ ), pertaining to spring, summer, and fall months, are around 700 W m<sup>-2</sup> and 15 °C, respectively (Table 2) [7]. For the said input solar radiation and for a given collector area of 1.15 m<sup>2</sup>, the collector useful heat gain ( $Q_u$ ) is estimated using the following equation:

$$Q_u = F' A_c [I_T (\alpha \tau) - U_L (T_f - T_a)]$$

**Table 2** Monthly solar radiation and ambient temperature data, 2012 [7]

Months	Solar radiation/W m <sup>-2</sup>	Ambient temperature/°C
March	675	5
April	759	8
May	828	15
June	930	21
July	967	21
Aug	861	23
Sept	569	20
Oct	356	13
Average	740	15

where  $I_T$  is the average hourly total solar radiation input,  $U_L$  is the heat loss coefficient of an evacuated tube collector ( $= 1 \text{ W m}^{-2} \text{ K}^{-1}$ ),  $T_f$  is the average working fluid temperature ( $= 45 \text{ }^\circ\text{C}$ ) [8] and  $F'$  is the collector efficiency factor ( $= 0.95$ ) (Table 3) [9]. For these input values, the useful heat gain turns out to be around  $600 \text{ W m}^{-2}$ .

*Confirmation Test:* The estimated useful heat gain is cross-checked by re-evaluating the net useful gain, using the following equation:

$$\eta_{\text{col}} = \frac{Q_u}{I_T A_c}$$

For the given collector area ( $= 1.15 \text{ m}^2$ ), average hourly total radiation ( $740 \text{ W m}^{-2}$ ), and the proven efficiency of the ETC of about 70% [10], the predicted useful heat gain (600 W) is in line with the previous estimated value.

Based on the above given values, it was decided to choose the diameter as 13'' (0.3 m) and height as 28'' (0.6 m), respectively. However, to accommodate the thermal expansion while water getting heated up as well as since it is indented to study the effect of mass of water as one of the operating parameters, the volume is set to 70 L. Accordingly, the storage tank was designed and built with a  $V = 70 \text{ L}$ ,  $D = 13''$  (0.3 m), and  $H = 31''$  (0.8 m).

The predicted useful heat gain (600 W) is utilized in identifying the required volume of the storage tank. Due to the domestic needs, the temperature of hot water ranges between  $60 \text{ }^\circ\text{C}$  and  $70 \text{ }^\circ\text{C}$ , and an average value of  $65 \text{ }^\circ\text{C}$  (Two) was tested in the design calculations. Similarly, the temperature of city water in Fargo ranges between  $15$  and  $20 \text{ }^\circ\text{C}$  [12] and hence  $T_{wi}$  ( $= 15 \text{ }^\circ\text{C}$ ) was used in the below given expression to evaluate the volume of the storage tank. With the above mentioned data for temperature rise of  $50 \text{ }^\circ\text{C}$ , the storage tank volume turns out to be 60 L, by evaluating following energy balance equation:

$$Q_u = V \rho C_{pw} (\Delta T)$$

**Table 3** Parameters used in the performance study [9, 11]

Thickness of copper fin ( $\delta$ )	0.0006 m
Circumference distance between U-tube (W)	0.108 m
Total solar isolation ( $I_T$ )	$740 \text{ W m}^{-2}$
Overall loss coefficient ( $U_L$ )	$1 \text{ W m}^{-2} \text{ K}^{-1}$
Bond conductance ( $C_B$ )	30
Collector efficiency factor ( $F'$ )	0.95
Fin efficiency of straight fin ( $F$ )	0.99
Acceleration due to gravity	$9.8 \text{ m s}^{-2}$
Thermal conductivity of water ( $k_w$ )	$0.58 \text{ W mK}^{-1}$
Specific heat of water ( $C_{pw}$ )	$4182 \text{ J kg}^{-1} \text{ K}$
Density of water ( $\rho_w$ )	$1000 \text{ kg m}^{-3}$

Having identified the volume of the storage tank, the optimal dimensions in terms of diameter and height was arrived based on the aspect ratio. Table 1 gives the aspects ratio for various assumed height and diameter for 60L. Having identified the volume of the storage tank, the optimal dimensions in terms of diameter and height were arrived based on the aspect ratio.

### Heat exchanger/condenser

Condenser coil is another important design element of the SWH system. In this study, an 'Indirect mode' and a heat exchanger (HX) are employed in order to transfer absorbed solar heat from the working fluid to the storage tank. For indirect water heating, an immersed coil-in-tank heat exchanger (Fig. 2) is designed using copper piping as it is more efficient, resistance to corrosion, and has good thermal conductivity [5].

A heat exchanger aids in facilitating the condensation of vapor by maximizing the heat rejection in the storage tank. This is largely influenced by the area of the condenser coil chosen. The methodology adopted in arriving at the area of the condenser coil is explained in this section.

### Determination of the heat exchanging/condenser area

The required condenser area was estimated based on the predicted average useful heat gain ( $Q_u$ ) by the collector during a typical one-day operation. It should be pointed out here that in design analysis, neglecting the pipe losses, it is assumed that the heat gained by  $\text{CO}_2$  at the evaporator (600 W) is expected to be same  $\text{CO}_2$  working fluid that is available at the condenser

$$Q_{\text{con}} = Q_u$$

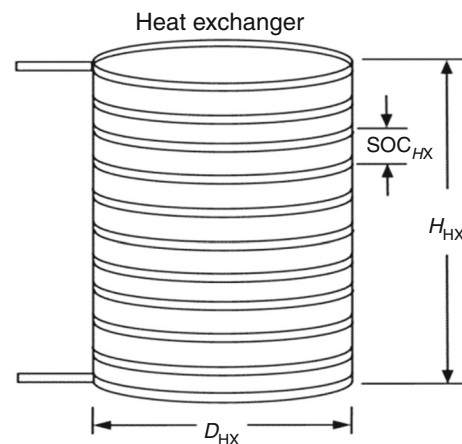


**Fig. 2** Picture and schematic of the designed condenser and the cooling coil

The heat rejected by the CO<sub>2</sub> through the condenser can be expressed as

$$Q_{\text{con}} = (UA)_{\text{coil}}(T_{\text{con}} - T_w)$$

where the area of the cooling coil and  $U_{\text{coil}}$  is the overall heat transfer from the condenser/cooling coil. The required total heat transfer area (cooling coil area) depends on the overall heat transfer coefficient ( $U_{\text{coil}}$ ). In general, the value of overall heat transfer coefficient varies considerably based on the thermal and transport properties of both fluids and on other conditions. The  $U_{\text{coil}}$  is given by [13]:

$$U_{\text{coil}} = \frac{1}{(B/h_{\text{co}})/(1/h_w)}$$

where  $B = 1$

The heat transfer coefficient ( $h_{\text{co}}$ ) of refrigerant inside the horizontal tubes during the condensation process for two-phase annular flow can be estimated using the following equation (Jordan and Priester [14]):

$$h_{\text{co}} = 0.025 \frac{k_r}{d_i} \left( \frac{G_r d_i}{\mu_r} \right)^{0.8} \left( \frac{C_{\text{pr}} \mu_r}{k_r} \right)^{0.3}$$

where  $G_r$  is the mass velocity for two-phase flow,  $k_r$  is the thermal conductivity of the refrigerant,  $C_{\text{pr}}$  is the specific heat of the refrigerant, and  $\mu_r$  is the dynamic viscosity of the refrigerant [13]. These properties are evaluated at the required condenser temperature ( $T_{\text{con}}$ ). As it is intended to build a SWH to meet the domestic hot water needs, in general the temperature varies from 60 to 70 °C [12]. Hence, design calculations at value of  $T_{\text{con}} = 65$  °C was used, and the heat transfer coefficient of the refrigerant ( $h_{\text{co}}$ ) turns out to be around 6000 W m<sup>-2</sup>.

Similarly, the water side heat transfer coefficient ( $h_w$ ) is estimated by using the following equation [13]:

$$h_w = 0.5 \frac{k_w}{d_o} \left( \frac{g \beta_w \Delta t d_o^3 \rho_w^2 C_{\text{pw}}}{\mu_w k_w} \right)^{0.25}$$

where  $k_w$  is the thermal conductivity of the water,  $g$  is the acceleration due to gravity,  $\beta_w$  is the coefficient of thermal expansion of water,  $C_{\text{pw}}$  is the specific heat of water, and  $\mu_w$  is the dynamic viscosity of water. These properties are evaluated at the water temperature ( $T_w$ ) of 15 °C, equivalent to the city water temperature in Fargo. The various properties of water and carbon dioxide and their variation with the designed temperature and pressure conditions are presented in Table 3 [13].

Substituting the overall heat transfer coefficient of the coil estimated useful heat gain (600 W), temperature of the condenser coil ( $T_{\text{con}} = 65$  °C) and the temperature of water in the tank ( $T_w = 15$  °C), the required surface area of the coil ( $A_{\text{coil}}$ ) turns out to be 0.04 m<sup>2</sup>.

### Determination of the coil length and number of turns of the coil

For the desired surface area of the coil (0.04 m<sup>2</sup>), and diameter of the coil (0.003 m), the overall length of the coil ( $L_{\text{coil}}$ ) turns out to be 5 m (196.8").

$$A_{\text{coil}} = \pi D_i L_{\text{coil}}$$

Depending upon the predicted overall length of the coil and the allowable diameter of the each turn, the number of turns can be evaluated. The turn diameter depends on the diameter of the storage tank. The chosen diameter of the tank was set to 13" (0.33 m). Hence, giving a clearance of 2.5" (0.06 m), from the inner wall of the tank, the allowable diameter of the each turn will be 8" (0.2 m). Therefore, for the given total cooling coil length → the possible number of turns will be nine turns.

In the view of effective heat transfer process from the condensing coil, it would be desirable to have the condenser coils be spaced in the tank which would enhance free convection currents. However, based on the chosen height (28") of the storage tank, the spread of the coil could not exceed the said height. However, giving a clearance of 7" on either side of the condensing unit, the coil could be spread within a height of 14" (0.35 m) only. This also ensures that the condenser coil is immersed well within the desired volume of storage water (60 L). It is well known that the condenser coil should be totally immersed in water, in order to take advantage of the greatest difference between the temperature of the storage fluid and the temperature of the fluid flowing through the condenser [16]. Based on this, the coil was located within the middle of the storage tank, with a clearance of 7" (0.17 m) at the either end of the tank. Depending on the height of the storage tank that is, 28" (0.71 m), the inlet and the outlet of the HX was set at the storage tank height of 21" (0.53 m) and 7" (0.17 m), respectively.

### Collector design

Generally, the main design variables that influence the collector effectiveness are: the collector type and collector size. An evacuated tube solar collector (ETC) was chosen as the heating device as they are a naturally fit for colder regions and proven to minimize heat losses [17]. The main two components of the ETC, i.e., U-tube and Header design, are discussed in below sections.

### U-tube design

The efficiency of a collector is also dictated by the shape of the absorber tube [18]. A study [19] introduced several potential designs of the absorber tube and investigated the



performance of the four different shapes of absorber tubes. The shapes include (1) a finned tube, (2) an “U-tube” welded inside a circular fin, (3) an “U-tube” welded on a copper plate. Among the different designs, an “U-tube” integrated with circular fin provided the best heat transfer performance. Based on the above information, an U-shaped absorber tube was designed, for the proposed ETC system.

In order to accommodate high operating pressures (8–13 MPa) experienced with CO<sub>2</sub> as the working fluid compared to any other conventional refrigerants in the temperature range of 20–90 °C [20], a copper tube of 15 mm thick and 3.7 m long was bent to U-shape and was inserted in the inner ETC tube to accommodate the abovementioned high-pressure CO<sub>2</sub>.

### Header design

As shown in Fig. 3, an input and output header pipes with an opposing 5° angle were designed to limit reverse flow.

This design will also aid in uniform flow in the collector. In order to handle the previously mentioned high-pressure CO<sub>2</sub>, copper tubing was chosen which had an outer and inner diameter of 0.009 m and 0.006 m, respectively, in the header area. The length of the header section was 0.609 m. Multiple stainless steel high-pressure compression T-joints were employed to join the copper tubes in the ETC with the headers.

### Data acquisition

The following section provides a description of the instrumentation procedure carried out in this study (Fig. 4).

J-type thermocouples were used to record water temperature in the storage tank and CO<sub>2</sub> temperature at various locations of the system. Figure 5 shows the picture of a thermocouple installed within the flow. Three sensors, at the inlet and outlet of the collector and within the storage tank, were inserted in the respective location by a T-joint into the copper tubing, and to seal the thermocouple at the

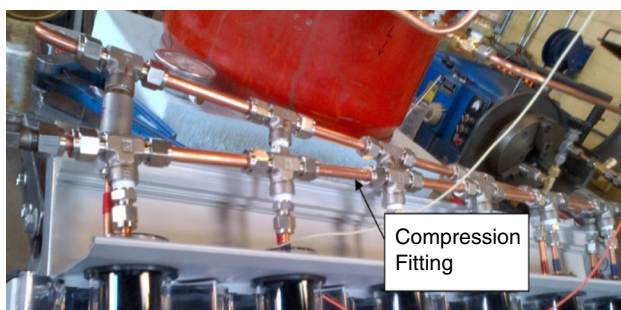


Fig. 3 Input and output header

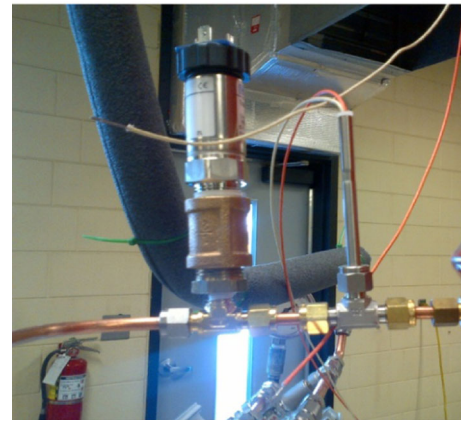
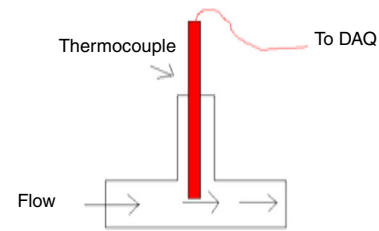


Fig. 4 Schematic and picture of temperature sensor installed into the flow

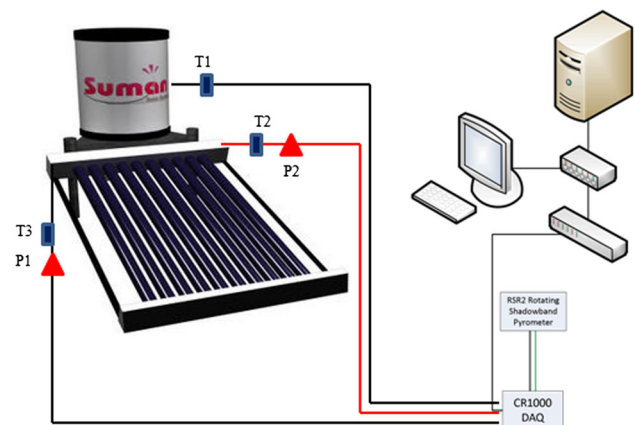


Fig. 5 System testing setup

given location, a compression Farrell fitting adaptor was used.

Similarly, special pressure sensors were used to measure the pressure of the refrigerant at the inlet and outlet of the heat exchangers. Two pressure transducers (Fig. 4), with a range of 0–15 MPa, were used at the inlet and the outlet of the heat exchanger. The pressure output for each of the sensors was in the range of 0–10 V.

The data measured were retrieved using RSR CR1000 logger net software from the various sensors as shown in Fig. 6.



Fig. 6 RSR CR1000 logger net software used in the prototype

## Results and discussions

Based on the design procedure described in the previous sections, a prototype of a simple thermosyphon SWH system using supercritical CO<sub>2</sub> as the working fluid was designed and installed at the North Dakota State University, Fargo. The experiments were carried out to study CO<sub>2</sub> characteristics in terms of temperature and pressure along with collector performance in severe cold conditions.

### Temperature and pressure of carbon dioxide in the collection system

The characteristics of supercritical CO<sub>2</sub>-based solar collector, including CO<sub>2</sub> temperature and pressure play an important role in dictating the overall performance of the proposed thermosyphon solar water heating system. Experiments were conducted to understand the nature of supercritical CO<sub>2</sub> in the collector.

The collection system consisting of a collector 1.15 m<sup>2</sup> exposed area was initially filled with CO<sub>2</sub>. The collector, kept facing south at the angle of 45° to the horizontal (equal to the latitude of Fargo), was exposed to solar radiation from 8:00 h. No carbon dioxide vapor was being used for the end uses purposes. The carbon dioxide in the system was allowed to be heated continuously by the thermosyphon action.

The temperatures of the carbon dioxide were periodically measured using J-type thermocouple at the inlet and the out of the collector. The high CO<sub>2</sub> pressures at various locations of the systems were measured, using pressure transmitters. The global radiation intensity incident on the collector surface was measured using solarimeter. The

above measuring processes were monitored and recorded at frequent intervals of time.

The  $I_T$  was taken as 775 W m<sup>-2</sup>, which is the maximum solar radiation intensity recorded by the solarimeter at the 14:00 h on the day of experiments. In the experiments, the collector was exposed to the sun at 08.00 h. Figure 7 shows the variation in CO<sub>2</sub> temperature with time. It is seen that temperature increases rapidly to begin with, the reason being (1) the intensity of the radiation on the collector increasing continuously and (2) the losses from the collector were small as the collector temperature was low initially.

After noon hours, the temperature increases slowly. This was because of the high losses from the collector due to the higher temperature in the system. Beyond 14.00 h, the increase was very small. Actually there should be a fall in temperature beyond 14.00 h as the radiation intensity was on decrease. But, the effect of reducing radiation is compensated until 15:00 h by the heat capacity effect of the collector and CO<sub>2</sub> in it. CO<sub>2</sub> reaches a maximum of 90 °C at around 15:00 h.

Figure 8 shows the corresponding variation of pressure with time. The CO<sub>2</sub> pressure varies largely with the solar radiation in the collector. A maximum pressure of around 13 Mpa was recorded at 15:00 h. Beyond 15.00 h, the temperature and pressure fall with the decrease in the solar radiation.

Based on the above discussion, it can be concluded that for CO<sub>2</sub>-based collector, not only the CO<sub>2</sub> temperature but also the CO<sub>2</sub> pressure in the collector was influenced by the solar radiation, which makes the collector characteristics more complicated than traditional collectors using water as working fluid.

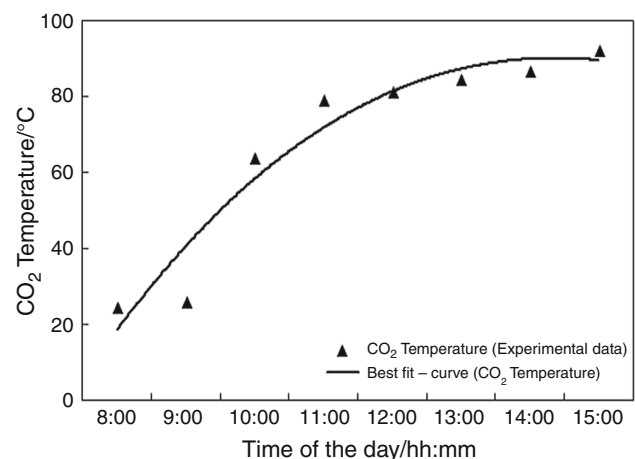


Fig. 7 Variation of CO<sub>2</sub> temperatures with time

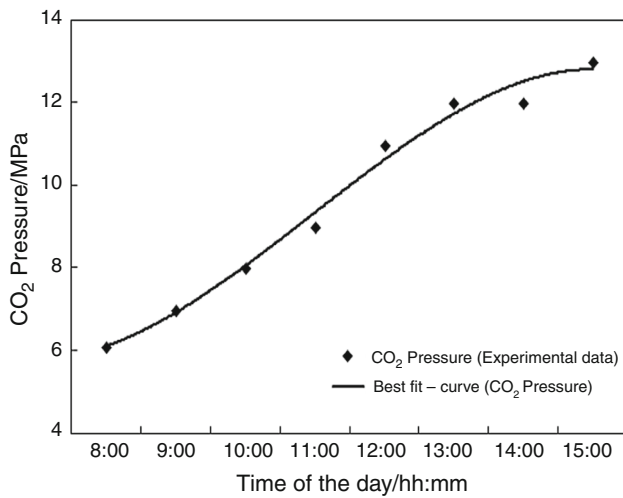


Fig. 8 Variation of CO<sub>2</sub> pressure with time

### Performance of Evacuated Tube Collector

The testing of the collector was conducted in such a way that an “efficiency curve” was determined for the collector under stagnation conditions. Experimental results were utilized to produce efficiency profile of evacuated tube U-pipe solar collector. The efficiency values calculated were plotted against parameter  $(T_f - T_a)/I_T$ . Figure 9 shows the efficiency varies profile of the evacuated tube U-pipe solar collector. The maximum global solar radiation intensity recorded by the solarimeter on the day of experiment was  $775 \text{ W m}^{-2}$ . As seen in Fig. 9, experimental data points are clearly scattered about the straight line.

Figure 9 also shows that efficiency reduces linearly with an increase in the parameter  $(T_f - T_a)/I_T$ . The slope of the profile is negative, as the difference between the working fluid and ambient temperature rises, the radiation and convection losses from the collector also increase. In general, as per the law of conservation of energy, the

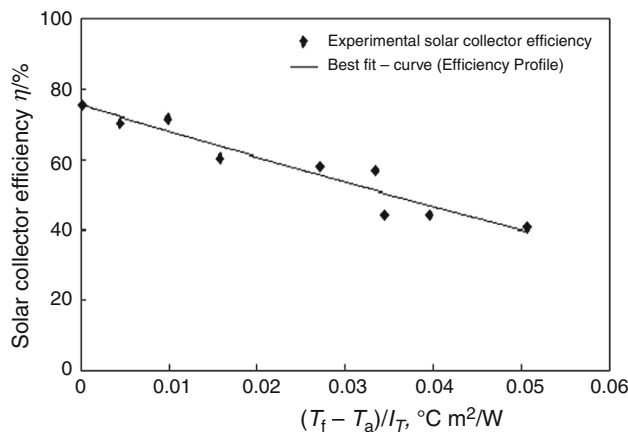


Fig. 9 Performance of an evacuated tube collector

Table 4 The parameters for the glass evacuated tube solar collector

Materials	Parameters	Value
Absorbing coating	Absorptivity	0.92
	Emissivity	0.19
Outer glass tube	Outer diameter/m	0.01
	Inner diameter/m	0.03
	Thickness/m	0.0015
Air layer	Conductivity/W $\text{mK}^{-1}$	1.2
	Thickness/m	0.001
	Conductivity/W $\text{mK}^{-1}$	0.03
Copper fin	Thickness/m	0.0006
	Conductivity/W $\text{mK}^{-1}$	307
U-tube	Outer diameter/m	0.0063
	Inner diameter/m	0.0031
	Thickness/m	0.015

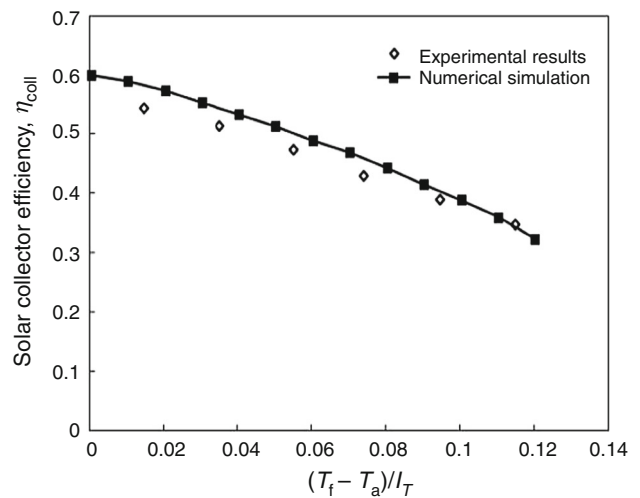


Fig. 10 Comparison between theoretical and experimental results of solar collector efficiency [22]

collector performance can be further improved by increasing energy transmission through the collector to the working fluid (useful energy) and minimizing the collector heat losses, with improved insulation techniques. Details of the collector been summarized are listed in Table 4.

A numerical model and simulation study has been developed and conducted by R Islam [21] to optimize the SWH system design. The study confirmed that both the solar radiation and ambient temperature have a significant impact on the SWH system’s thermal performance.

The author verified the simulation results with the experimental results conducted during a sunny day (in this study) and examined the variation in collector efficiency [22]. As indicated earlier in Fig. 9, experimental data points are clearly scattered about the straight line which

confirms that the collector efficiency agrees well with the simulation results (Fig. 10).

## Conclusions

The detailed design analysis of a simple thermosyphon SWH system is discussed in this study. The components such as storage tank, heat exchanger, and collector U-tube design were fabricated and designed to ensure the functioning of SWH system in North Dakota, USA weather conditions. The experimental results indicated that in severe cold conditions, existing SWH heating is not so effective. However, the collector design and as heat transfer fluid showed promising and potential results when operated in solar adverse regions. This is due to the thermodynamic and transport properties of CO<sub>2</sub> seem to be favorable in terms of heat transfer and pressure drop. In such severe cold condition, a recommendation is made to study heat pump-assisted solar water heating system (using CO<sub>2</sub>) to improve system's efficiency.

## References

1. Sawin J, Seyboth K, Sverrisson F. REN21's Renewables Global Status Report 2016. REN21. 2016
2. Yao C, Haoa B, Liua S, Chen X Analysis for common problems in solar domestic hot water system field-testing in China. In: International conference on solar heating and cooling for buildings and industry, SHC 2014. Energy Procedia 2015; vol 70, pp 402–408
3. Srivastava U, Malhotra RK, Kaushik SC. Review of heat transfer properties of solar heat transfer fluids. J Therm Anal Calorim. 2017;130:605–21.
4. Pandey AK, Tyagi VV, Rahim NA, Kaushik SC. Thermal performance evaluation of direct flow solar water heating system using exergetic approach. J Therm Anal Calorim. 2015;121:1365–73.
5. Shukla R, Sumathy K, Erickson P, Gong J. Recent advances in the solar water heating systems: a review. Renew Sustain Energy Rev. 2013;19:173–90.
6. Abdunnabi MJR, Loveday DL Optimization of Thermosyphon Solar Water Heaters Using TRNSYS.Part2: Parametric.
7. Study Using a Modified TRNSYS Model, International Conference on Future Environment and Energy.
8. <http://ndawn.ndsu.nodak.edu/>.
9. H. Yamaguchi, N. Sawada, H. Suzuki, H. Ueda, X. R. Zhang. Preliminary Study on a solar water heater using supercritical Carbon dioxide as working fluid. J Solar Energy Eng (2010). <https://doi.org/10.1115/1.4000350>
10. Ma L, Lu Z, Zhang J, Liang R. Thermal performance analysis of the glass evacuated tube solar collector with U-tube. Build Environ. 2010;45:1959–67.
11. <http://www.energymatters.com.au/renewable-energy/solar-power/solar-hot-water/flat-vs-evacuated.php>.
12. Austin BT, Sumathy K. Parametric study on the performance of a direct expansion geothermal heat pump using carbon-dioxide. Appl Therm Eng. 2011;31:3774–82.
13. [http://www.engineeringtoolbox.com/design-hot-water-system-d\\_92.html](http://www.engineeringtoolbox.com/design-hot-water-system-d_92.html).
14. Kuang YH, Sumathy K, Wang RZ. Study on a direct –expansion solar assisted heat pump water heating system. Int J Energy Res. 2003;27:531–48.
15. Jordan RC, Priestler GB. Refrigeration and air conditioning. New York: Prentice-Hall Inc; 1948.
16. [http://www.engineeringtoolbox.com/heat-transfer-coefficients-exchangers\\_d450.html](http://www.engineeringtoolbox.com/heat-transfer-coefficients-exchangers_d450.html).
17. Dahm J, Bales C, Lorenz K, Dalenba J-O. Evaluation of storage configuration with internal heat exchanger. Sol Energy. 1998;62:407–17.
18. <http://www.energymatters.com.au/renewable-energy/solar-power/solar-hot-water/flat-vs-evacuated.php>.
19. Perez R, Seals R, Anderson J, Menicucci D. Calculating solar radiation received by tubular collectors. J Sol Energy Eng. 1995;117:341–4.
20. Kim Y, Seo T. Thermal performances comparisons of the glass evacuated tube solar collectors with shapes of absorber tube. Renew Energy. 2007;95:772–95.
21. R Islam. Numerical simulation of direct expansion solar assisted heat pump water heater using carbon dioxide as refrigerant. North Dakota State University of Agriculture and applied science, 2013.
22. Zhang XR, Yamaguchi H. An experimental study on evacuated tube solar collector using supercritical CO<sub>2</sub>. Appl Therm Eng. 2008;28:1225–33.